J. Dairy Sci. 102:1–15
https://doi.org/10.3168/jds.2018-15906

Candidate genes associated with the heritable humoral response to *Mycobacterium avium* subspecies *paratuberculosis* in dairy cows have factors in common with gastrointestinal diseases in humans

S. P. McGovern,[1] D. C. Purfield,[2] S. C. Ring,[3] T. R. Carthy,[2] D. A. Graham,[4] and D. P. Berry[2]*
[1]Department of Microbiology, University College Cork, Coláiste na hOllscoile Corcaigh, College Road, Cork City, Co. Cork, Ireland T12CY82
[2]Teagasc, Animal & Grassland Research and Innovation Centre, Moorepark, Fermoy, Co. Cork, Ireland P61C996
[3]Irish Cattle Breeding Federation, Highfield House, Shinagh, Bandon, Co. Cork, Ireland P72 X050
[4]Animal Health Ireland, 4-5 The Archways, Carrick-on-Shannon, Co. Leitrim, Ireland N41WN27

ABSTRACT

Infection of cattle with bovine paratuberculosis (i.e., Johne's disease) is caused by *Mycobacterium avium* subspecies *paratuberculosis* (MAP) and results in a chronic incurable gastroenteritis. This disease, which has economic ramifications for the cattle industry, is increasing in detected prevalence globally; subclinically infected animals can silently shed the bacterium into the environment for years, exposing contemporaries and hampering disease-control programs. The objective of the present study was to first quantify the genetic parameters for humoral response to MAP in dairy cattle. This was followed by a genome-based association analysis and subsequent downstream bioinformatic analyses from imputed whole genome sequence SNP data. After edits, ELISA test records were available on 136,767 cows; analyses were also undertaken on a subset of 33,818 of these animals from herds with at least 5 MAP ELISA-positive cows, with at least 1 of those positive cows being homebred. Variance components were estimated using univariate animal and sire linear mixed models. The heritability calculated from the animal model for humoral response to MAP using alternative phenotype definitions varied from 0.02 (standard error = 0.003) to 0.05 (standard error = 0.008). The genome-based associations were undertaken within a mixed model framework using weighted deregressed estimated breeding values as a dependent variable on 1,883 phenotyped animals that were ≥87.5% Holstein-Friesian. Putative susceptibility quantitative trait loci (QTL) were identified on *Bos taurus* autosome 1, 3, 5, 6, 8, 9, 10, 11, 13, 14, 18, 21, 23, 25, 26, 27, and 29; mapping the most significant SNP to genes within and overlapping these QTL revealed that the most significant associations were with the 10 functional candidate genes *KALRN*, *ZBTB20*, *LPP*, *SLA2*, *FI3A1*, *LRCH3*, *DNAJC6*, *ZDHHC14*, *SNX1*, and *HAS2*. Pathway analysis failed to reveal significantly enriched biological pathways, when both bovine-specific pathway data and human ortholog data were taken into account. The existence of genetic variation for MAP susceptibility in a large data set of dairy cows signifies the potential of breeding programs for reducing MAP susceptibility. Furthermore, the identification of susceptible QTL facilitates greater biological understanding of bovine paratuberculosis and potential therapeutic targets for future investigation. The novel molecular similarities identified between bovine paratuberculosis and human inflammatory bowel disease suggest potential for human therapeutic interventions to be translated to veterinary medicine and vice versa.

Key words: Johne's disease, resistance, quantitative trait loci, genome-wide association study, sequence

INTRODUCTION

Paratuberculosis, also known as Johne's disease, caused by the gram-positive aerobic bacterium *Mycobacterium avium* subspecies *paratuberculosis* (**MAP**), is a contagious disease primarily affecting ruminants. Paratuberculosis results in chronic, progressive gastroenteritis for which there is no cure (Harris and Barletta, 2001). First reported in Europe by Johne and Frothingham (1895) as a "peculiar case of tuberculosis in cattle," MAP is primarily spread via the fecal-oral route; younger animals are most susceptible to clinical MAP infection upon exposure (Windsor and Whittington, 2010). Clinical signs of MAP infection in cattle, primarily observed in older cattle (MAP has an incubation period of up to 10 yr; Collins, 2003), include weight loss due to characteristic pipe stream diarrhea, hypoproteinemia (Sweeney et al., 2012), reduced milk

Received October 26, 2018.
Accepted January 20, 2019.
*Corresponding author: Donagh.Berry@teagasc.ie

yield (Richardson and More, 2009), and reduced cull cow value (Richardson and More, 2009), all of which adversely affect both animal well-being and farm profitability. Infected animals silently shed MAP in their environment via contaminated feces, spreading paratuberculosis to uninfected animals (Koets et al., 2015).

Testing for MAP infection, concurrent with management (including measures to address both biocontainment and bioexclusion at the herd level) and vaccination strategies, are the advocated control measures used to curtail the spread of bovine paratuberculosis. Unfortunately, all of these have limited efficacy and will not guarantee eradication, even at the herd level, despite continued effort over an extended period. Correctly classifying animals as infected with paratuberculosis is challenging due to the available tests being suboptimal in both sensitivity and specificity; moreover, vaccination does not result in a reduction in the number of infected animals or offer long-term immunity (Park and Yoo, 2016; Geraghty et al., 2014). In addition, vaccination against MAP is prohibited in some countries (e.g., the Republic of Ireland). Previous studies on the contribution of genetic variability to paratuberculosis in dairy cattle suggest heritability estimates of susceptibility to the disease ranging from <0.01 (Koets et al., 1999) to 0.283 (Küpper et al., 2012). Differences in parameter estimates among studies could be due to a multitude of reasons, including the extent of variability (residual and genetic) in the populations sampled, sample sizes, trait definition, and models used (i.e., linear, threshold, animal, sire). Nonetheless, the nonzero heritability estimates of MAP susceptibility, coupled with the existence of considerable genetic variability, suggest that genetic selection could improve resistance to MAP infection in the bovine population; this could prove useful in the control and eradication of the disease concomitant with other control measures already in place.

Prior studies based on genome-wide associations (Settles et al., 2009; Pant et al., 2010; Alpay et al., 2014) have identified multiple different loci putatively associated with bovine paratuberculosis. The degree of concordance in reported QTL across studies is, however, poor. Only one study exists that used imputed whole-genome SNP data to detect loci associated with MAP infection in cattle, although the study was based on relatively small cohorts of up to 459 dairy cattle (Kiser et al., 2017). Kiser et al. (2017) identified loci on chromosomes 3, 8, 10, 12, 14, 16, 21, and 22 associated with paratuberculosis susceptibility. Three studies exist that have used a gene set enrichment analysis approach following a genome-based association analysis to investigate modest effect SNP and genes, enriched pathways, and gene ontologies associated with MAP infection in cattle (Neibergs et al., 2010; Del Corvo et al., 2017; Kiser et al., 2017).

The objective of the present study was to quantify the genetic parameters of the humoral response to MAP infection in a large cohort of Irish dairy cows. The derived parameters were subsequently used to estimate breeding values as an input variable for an association analyses using imputed whole-genome SNP data to detect regions of the bovine genome putatively associated with humoral response to MAP. The biology underpinning the detected regions was further investigated by conducting bioinformatics analyses to identify the underlying gene functions and related biochemical pathways.

MATERIALS AND METHODS

The data used in the present study were obtained from a pre-existing database managed by the Irish Cattle Breeding Federation (ICBF, Bandon, Co. Cork, Ireland). Therefore, it was not necessary to obtain animal care and use committee approval in advance of conducting this study.

Data

A total of 663,719 ELISA test records on humoral (blood and milk antibody) response to MAP were available from 9 Irish laboratories between June 2012 and November 2017, inclusive of 282,396 cows in 2,704 dairy and beef herds. The health status of these herds for other diseases was unknown. Only cows aged between 2 and 12 yr at the time of testing were considered. Records classified as inconclusive (n = 3,639), suspect (n = 1,406), or low positive (n = 4,210) were not considered further. Subsequently, all individual cow test records were classified as either positive (13,685 records) or negative (640,779 records) to MAP infection based on the respective test manufacturer's guidelines [Bovine ELISA Paratuberculosis Antibody Screening Kit (Institut Pourquier, Montpellier, France), ID Screen Paratuberculosis Indirect Screening Test (ID Vet, Montpellier, France), *Mycobacterium paratuberculosis* Antibody Test Kit PARACHEK (Prionics, Zurich, Switzerland) and Paratuberculosis Antibody Screening Test (Idexx Laboratories, Westbrook, ME)].

Of the 10,137 cows with at least 1 positive ELISA record, 2,651 also had a negative MAP result following a positive MAP result; these cows were discarded from the data set. Only data from dairy herds were considered further. A herd was classified as beef or dairy based on the average breed composition of the cows, as per Twomey et al. (2016). Cow breed composition

was determined from the recorded breed composition of ancestors. A dairy herd was defined as a herd whose average dairy breed proportion of the cows was ≥75%. Only herd-years with ≥25 cows tested were retained. Following these edits, 612,375 test records from 260,740 cows in 4,543 herd-years from 2,170 herds remained.

Herd-years defined as MAP naïve were those which only had MAP-negative cattle residing in them; these herd-years were not considered further, leaving a total of 378,701 records from 186,174 cows in 2,485 herd-years (1,487 herds). The remaining herd-years were considered exposed to MAP infection, as they had at least 1 cow that yielded an ELISA-positive result. To be retained, all cows must have calved at least once in the herd before being tested in the positive herd-year. All cow interlocation movement data were available from the ICBF database, as it is a legal requirement to record these movements in Ireland. A cow was considered exposed to MAP if she resided in an exposed herd-year for at least 1 yr before an ELISA test. This was to allow MAP-negative cows adequate time to become exposed to MAP via infected contemporary(ies).

Cow parity at test was categorized as 1, 2, 3, 4, or ≥5. Stage of lactation (i.e., DIM) at ELISA test was categorized into 9 categories: 10 to 49, 50 to 99, …, and 400 to 450; cows <10 or >450 DIM at test were not considered further. Cows with no sire information were discarded, and only the most recent test result per cow was considered further. Following these edits, 155,072 cows remained. General heterosis and recombination loss coefficients for each animal were calculated as $1-\sum_{i=1}^{n}\text{sire}_i \times \text{dam}_i$ and $1-\sum_{i=1}^{n}\frac{\text{sire}_i^2 \times \text{dam}_i^2}{2}$, respectively, where sire_i and dam_i are the proportion of breed i in the sire and dam, respectively (VanRaden and Sanders, 2003).

Contemporary groups were defined as herd-year-season of test using an algorithm described in detail by Berry and Evans (2014). The algorithm clusters herd contemporaries that were tested around the same period of the year together but within no more than 90 d of each other. Only contemporary groups with at least 5 cows and at least 1 positive and 1 negative MAP test result were retained. After edits, the final data set comprised 136,767 cows from 2,463 herd-years with test records reported from 8 different laboratories.

Genetic Parameter Estimation and Genetic Evaluation

Variance components for humoral response to MAP were estimated using animal and sire linear mixed models in ASReml (Gilmour et al., 2009). The fitted linear mixed model was

$$Y = CG + \textit{heterosis} + \textit{recombination} + \textit{parity} \times \textit{stage of lactation} + a + e,$$

where Y is the binary dependent variable of the MAP phenotype; CG is the fixed effect of contemporary group; *heterosis* is the fixed effect of a general heterosis coefficient (0.0%, >0.0 to <0.1%, ≥0.1 to <0.2%, …, ≥0.9 to <100%, 100%); *recombination* is the fixed effect of a general recombination loss coefficient (0.00%, >0.00 to <0.05%, ≥0.05 to <0.10%, …, ≥0.45 to <0.50%, 0.50%, >0.50%); *parity* is the fixed effect of the parity of the cow; *stage of lactation* is the fixed effect of stage of lactation; a is the random additive genetic effect of the animal where $a \sim N\left(0, \mathbf{A}\sigma_a^2\right)$, with σ_a^2 representing the additive genetic variance of the animal and $\mathbf{A}$ is the additive genetic relationship matrix among animals; and e is the random residual effect where $e \sim N\left(0, \mathbf{I}\sigma_e^2\right)$, with σ_e^2 representing the residual variance and $\mathbf{I}$ representing the identity matrix. Each cow's pedigree was traced back to the founder population, which was assigned to 1 of 10 genetic groups. Sire models used were as described above, except that the direct animal genetic effect was replaced by a sire genetic effect.

Genetic parameters were calculated for the overall data set of 136,767 cows, but also within each of the 8 laboratories separately. Genetic parameters were also estimated for humoral response to MAP, where the data were restricted to 33,818 cows that resided in herd-years that contained at least 5 MAP ELISA-positive cows, with at least 1 of those positive cows being homebred. The observed binary scale heritability estimates were transformed to the underlying liability scale via the formula of Robertson and Lerner (1949) using the average MAP prevalence of the respective cohort:

$$h_L^2 = h_O^2\left[\frac{p(1-p)}{z^2}\right],$$

where h_L^2 is heritability on the liability scale (i.e., threshold model); h_O^2 is heritability on the observed scale; p is the trait prevalence/100; and z^2 is the height of the ordinate of the normal distribution corresponding to a truncation point applied to p.

Two genetic evaluations were conducted for the present study, the first for validating EBV and the second

for subsequent use in the genome-wide association analyses. Estimated breeding values and their corresponding reliabilities for MAP susceptibility were calculated using the MiX99 software suite (Strandén and Lidauer, 1999) with the fitted animal model being the same as previously described. The EBV were estimated for the set of 33,818 phenotyped cows and their relatives that resided in herd-years that contained at least 5 MAP-positive cows, with at least 1 of those positive cows being homebred.

Validation of EBV

For the purposes of validation of the genetic evaluations, the MAP phenotype of a subcohort of the 33,818 cows was masked and their breeding values estimated via their pedigree links with related phenotyped animals. The validation data set was chosen based on herd-year characteristics in that only herd-years with at least 20 phenotyped animals and a mean herd incidence of between 10 and 25% were retained. In total, 6,600 animals from 94 herds were considered in the validation; the mean prevalence of ELISA positivity in this cohort was 15%. Once the MAP phenotypes were masked, a genetic evaluation was undertaken using the phenotypes of all remaining 27,218 animals. The EBV of the validation animals with an estimated reliability of >0.05 were retained; 5,477 animals remained. Within herd-year, the validation animals were stratified equally (where the modular of 3 per herd was 0, otherwise as close to equal as possible) into high EBV (poor), average EBV, and low EBV (good) groups. Logistic regression was used to model the association between EBV stratum (n = 3) and the logit of the probability of a positive MAP outcome; a binomial distribution of errors was assumed. The area under the receiver operating curve was estimated and the odds of a positive outcome calculated from the model solutions; the low EBV group was used as the referent category. A further logistic regression analysis was undertaken where the fixed effects model terms of herd-year, heterosis, recombination, and a 2-way interaction between parity and stage of lactation were also fitted.

Whole-Genome Sequence Imputation and Association Analysis

Of the 433,989 animals with an EBV from the genetic evaluation (with no masked phenotypes), only genotyped animals ≥87.5% Holstein-Friesian were considered for the genome-wide analysis. Principal component analysis of the genotypes (along with animals from other breeds) was used to ensure all animals were Holstein-Friesian; 8,780 animals remained. The EBV estimated for the Holstein-Friesian animals were deregressed using the Secant method in MiX99 (Strandén and Mäntysaari, 2010) and, subsequently, effective record contributions were calculated for each animal. Only the subset of 1,883 genotyped animals (662 male, 1,221 female) that had an effective record contributions value ≥1 were considered further. These animals were initially genotyped using 1 of 7 Illumina arrays (Illumina Inc., San Diego, CA), namely 3k (2,909 SNP, n = 36), low density (7,931 SNP, n = 230), Bovine SNP50 (54,001 SNP, n = 300), International Dairy and Beef version 1 (IDBv1; 17,137 SNP, n = 121), IDBv2 (18,004 SNP, n = 677), IDBv3 (53,450 SNP, n = 236), and high density (777,962, n = 283). All animals had a call rate ≥90% and only autosomal SNP, SNP with a reported position as on UMDv3.1, and SNP with a call rate ≥90% were retained within each panel.

All animals were imputed to high density using a 2-step approach with FImpute2 software (Sargolzaei et al., 2014); this involved imputing the International Dairy and Beef, low density, and 3k genotyped animals to the Bovine50 beadchip density (i.e., 54,001 SNP) and, consequently, imputing all resulting genotypes (including the Bovine50 Beadchip genotypes) to high density using a multibreed reference population of 5,504 high-density genotyped animals. The genotypes of all animals were imputed to whole-genome sequence level using a reference population of 2,333 *Bos taurus* animals (using multiple breeds) from Run6.0 of the 1,000 Bulls Genomes Project (Daetwyler et al., 2014). A consensus SNP density across all animals was achieved using SAMtools version 1.3.1 (Li, 2011), followed by Beagle software version 4.1 imputation (Browning and Browning, 2016) to call variants in the reference population and improve genotype calls. Details of the alignment to UMDv3.1, variant calling, and quality controls conducted on the reference population are described by (Daetwyler et al., 2014). A total of 41.39 million SNP variants were called with an average coverage of 12.85×. The imputation procedure was completed by initially using Eagle v2.3.2 (Loh et al., 2016) to phase imputed high-density genotypes, followed by imputation to whole-genome sequence level using minimac3 (Das et al., 2016).

Regions of poor whole genome sequencing imputation accuracy, perhaps due to local misassemblies or misoriented contigs, were identified using an additional data set of 147,309 verified parent-progeny relationships. Mendelian errors, defined as the proportion of opposing homozygotes in a parent-progeny pair, were estimated for each relationship and the subsequent Mendelian error rate per SNP was determined. To accurately identify genomic regions of poor imputation, the R package GenWin (Beissinger et al., 2015), which

fits a β-spline to the data to find likely inflection points, was used to determine genomic region breakpoints of high Mendelian errors. Windows were analyzed using an initial window size of 5 kb and Genwin-pooled windows for which the SNP Mendelian error rate were similar. The average SNP Mendelian error rate per window was estimated and all variants within windows where the mean SNP Mendelian error rate was >0.02 were removed (687,137 SNP were removed).

A genomic relationship matrix, using just the autosomal high-density SNP genotypes, was constructed among animals using the VanRaden method 1 (VanRaden, 2008). Association analyses were undertaken for each SNP separately, using linear mixed models in WOMBAT (Meyer, 2007) to calculate SNP effects for all 1,883 animals. The model fitted for each SNP analysis was

$$Deregressed\ EBV = \mu + SNP + a + e,$$

where *deregressed EBV* is the dependent variable; μ is the fixed effect of the population mean; *SNP* is the fixed effect of allele dosage for each SNP (coded as 0, 1, or 2); a is the random effect of the animal, where $a \sim N\left(0, \mathbf{G}\sigma_a^2\right)$, with σ_a^2 representing the additive genetic variance of the animal and $\mathbf{G}$ the genomic relationship matrix among animals; e represents the residual, where $e \sim N\left(0, \mathbf{I}\sigma_e^2\right)$, with σ_e^2 representing the residual variance and $\mathbf{I}$ the identity matrix. The dependent variable was weighted using the formula by Garrick et al. (2009):

$$w_i = \frac{1-h^2}{\left[c + \frac{1-r_i^2}{r_i^2}\right]h^2},$$

where w_i is the weighting factor of the deregressed EBV of the ith animal; h^2 is the heritability estimate (i.e., $h^2 = 0.05$ as estimated in the present study); r_i^2 is the reliability of the deregressed EBV for the ith animal; and c is the genetic variance not accounted for by the SNP (i.e., $c = 0.90$). Test statistics for all SNP were obtained and SNP with $P \leq 5 \times 10^{-8}$ were considered to be genome-wide significant.

Defining QTL

Genome-wide significant SNP ($P \leq 5 \times 10^{-8}$) informed the initial positions for QTL regions associated with humoral response to MAP. The QTL start and end positions were defined based on SNP that were in strong linkage disequilibrium (**LD**) with these significantly associated SNP. A squared correlation threshold value of ≥0.7 was used to define whether or not SNP were in strong LD with the significantly associated SNP. The QTL boundaries were defined as being the SNP within a 5-Mb window from the significantly associated SNP that passed the LD threshold. In cases where QTL boundaries were overlapping, these QTL were merged and considered as a single (larger) QTL.

Downstream Bioinformatic Analyses

Once defined, the QTL were subsequently mined for the presence of annotated candidate genes using Ensembl (https://www.ensembl.org/) based on the UMDv3.1 genome build (https://ccb.jhu.edu/bos_taurus_assembly.shtml). Only nonintergenic SNP were considered for further analysis; that is, SNP with annotation information for intron variant, splice donor variant, stop gained variant, missense variant, synonymous variant, downstream gene variant, or upstream gene variant. Pathway analyses were then conducted based on these identified candidate genes using InnateDB (http://www.innatedb.com/; Breuer et al., 2013), which used integrated pathway data from the Reactome Pathway Knowledgebase (https://reactome.org/; Fabregat et al., 2018), and the Pathway Interaction Database (Schaefer et al., 2009). The hypergeometric algorithm and Benjamini-Hochberg correction were used for querying InnateDB.

RESULTS

Variance Components

The prevalence of positive humoral response to MAP in the overall edited national cow data, which included 136,767 cows, was 4.0%; in the restricted cohort of 33,818 cows it was 7.7% and ranged from 3.1 to 5.5% among the 8 different laboratories (Table 1). For the animal models, heritability estimates ranged from 0.006 to 0.084 (Table 1); heritability estimates for the sire models ranged from 0.022 to 0.046. The heritability estimate for the overall population of 136,767 animals was 0.020 (SE = 0.003). The heritability estimate for the cohort of 33,818 animals that were subsequently used for the genomic analysis was 0.050 (SE = 0.008). The additive genetic standard deviation for the prevalence of positive humoral response to MAP in the 10 (i.e., data from 8 laboratories and either the full or reduced data set) different data sets ranged from 0.014 to 0.058 (Table 1). The additive genetic standard deviation for humoral response to MAP in the overall population was 0.027; the additive genetic standard deviation for the reduced cohort used for genomic analysis was 0.058.

Table 1. Summary statistics for *Mycobacterium avium* subspecies *paratuberculosis* infection for each cohort investigated[1]

Cohort	No. of animals	Prevalence (%)	σ_a	h^2 (SE)	h_L^2
Entire data set[2]	136,767	0.04	0.027	0.02 (0.003)	0.1014
Entire data set[3]	136,767 (7,105 sires)	0.04	0.114	0.02	0.1132
5 Positive, 1 homebred[2]	33,818	0.077	0.058	0.05 (0.008)	0.1721
5 Positive, 1 homebred[3]	33,818 (2,692 sires)	0.077	0.057	0.046	0.1572
Laboratory 1[2]	33,727	0.045	0.025	0.016 (0.005)	0.0770
Laboratory 2[2]	24,377	0.055	0.033	0.02 (0.008)	0.0937
Laboratory 3[2]	22,546	0.031	0.023	0.018 (0.006)	0.1141
Laboratory 4[2]	19,838	0.038	0.054	0.084 (0.013)	0.4536
Laboratory 5[2]	17,972	0.031	0.014	0.0063 (0.006)	0.0388
Laboratory 6[2]	5,433	0.055	0.021	0.009 (0.015)	0.0381
Laboratory 7[2]	10,197	0.029	0.018	0.012 (0.0095)	0.0731
Laboratory 8[2]	2,260	0.055	0.036	0.025 (0.032)	0.1039

[1]σ_a = additive genetic standard deviation; h_L^2 = transformed heritability on the liability scale.
[2]Animal model used.
[3]Sire model used.

EBV and Their Validation

The mean EBV reliability of the 433,989 animals (i.e., the 33,818 with MAP humoral phenotypes and their 400,171 nonphenotyped relatives) was 0.089 (SD = 0.087). The EBV of individual animals ranged from −0.190 to 0.159; the maximum EBV reliability was 0.92. Considering only the cows that had their own MAP phenotype available (i.e., the restricted cohort of 33,818 cows), the mean EBV reliability was 0.192 (SD = 0.058).

Summary statistics relating to the validation of EBV are in Table 2. The raw mean prevalences of MAP in the poor, average, and good EBV strata were 0.16, 0.14, and 0.12, respectively. The mean reliability of the EBV was similar for each stratum (poor = 0.149, average = 0.144, good = 0.143). Stratum for MAP EBV was associated ($P \leq 0.001$) with the logit of the probability of a positive MAP outcome; the area under the receiver operating curve when just MAP EBV stratum was included in the logistic regression was 0.539. Irrespective of whether only MAP stratum was included in the model or whether MAP stratum was also included simultaneously with other fixed effects, the poor EBV stratum had a greater ($P < 0.05$) odds (1.37 to 1.43) of having a positive MAP outcome, relative to the good EBV stratum. Although numerically worse, the odds of a positive MAP outcome in the animals within the average EBV stratum did not differ significantly from the good EBV stratum. The predicted probability of a positive MAP outcome in the poor, average, and good EBV strata for a third-parity cow, 100 to 149 DIM, with no heterosis or recombination in the average herd-year was 0.134, 0.115, and 0.101, respectively.

Genome-Based Associations and Downstream Bioinformatic Analyses

A Manhattan plot depicting the association between each SNP and the deregressed EBV phenotype for MAP humoral response is presented in Figure 1. The present study identified 223 SNP as being associated ($P \leq 5 \times 10^{-8}$) with MAP humoral response. A total of 17,960 SNP were identified as being in strong LD with these 223 SNP, resulting in 18,181 SNP considered as being associated with MAP humoral response. These SNP resided within 47 QTL regions, which were distributed across 17 chromosomes, namely BTA 1, 3, 5, 6, 8, 9, 10, 11, 13, 14, 18, 21, 23, 25, 26, 27, and 29 (Table 3). The chromosome that harbored the most QTL was BTA1 (10 QTL), the largest of the QTL being 6.87 Mb in length. Mining these 47 QTL regions for SNP annotation data and candidate genes resulted in 623 positional candidate genes identified for further investigation; further information on these findings can be found in Supplemental Table S1 (https://doi.org/

Table 2. Summary statistics and odds ratios (95% CI in parentheses) for animals stratified on EBV for *Mycobacterium avium* subspecies *paratuberculosis*

EBV stratum	No. of animals	Prevalence (%)	EBV (SD)	Reliability (SD)	Simple logistic regression odds (95% CI)	Multiple logistic regression odds (95% CI)
Poor EBV	1,812	0.16	0.019 (0.015)	0.15 (0.059)	1.43 (1.18, 1.72)	1.37 (1.13, 1.67)
Average EBV	1,816	0.14	0.002 (0.009)	0.14 (0.062)	1.19 (0.98, 1.44)	1.16 (0.95, 1.42)
Good EBV	1,849	0.12	−0.011 (0.009)	0.14 (0.063)	1	1

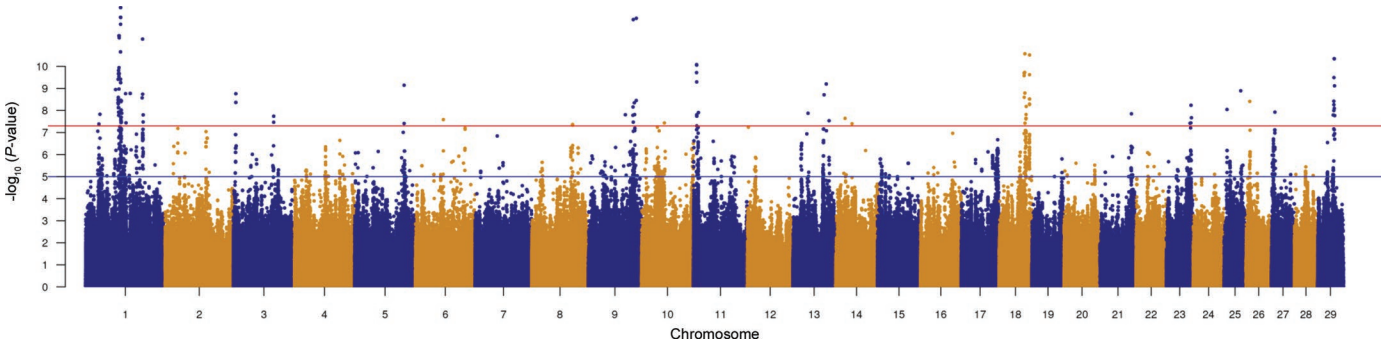

Figure 1. Manhattan plot of the sequence genome-wide association study using the deregressed EBV for humoral response to *Mycobacterium avium* subspecies *paratuberculosis*. These animals had an effective record contribution ≥1 (n = 1,883). Red threshold line = genome-wide significance (*P*-value $\leq 5 \times 10^{-8}$), blue threshold line = suggestive SNP (*P*-value $\leq 1 \times 10^{-5}$).

10.3168/jds.2018-15906). Of the 623 genes, the majority (301) were on BTA 18 (Table 3). The single QTL that harbored the most annotated positional candidate genes was on BTA 18 (from 53,905,719–61,291,660 bp; 243 genes), which contains genes such as *PKD2*, *HIF3A*, and *KLK1*.

The QTL that harbored the most genome-wide significantly associated SNP was on BTA 1 (from 70,108,608–71,811,570 bp), with 65 SNP identified and a further 14,543 in strong LD, and was 1.7 Mb long. The 5 most significantly associated SNP with MAP resistance resided in a QTL upstream of the QTL that harbored the most significantly associated SNP on BTA 1 (SNP genome-wide threshold *P*-value = 2.137×10^{-13}) and all within a range of 16.7 kb of each other. These SNP were all mapped to the Kalirin (*KALRN*) gene: 4 were intronic variants (rs378864226, rs719379694, rs37959091, and rs384286217) and 1 was identified as a splice donor variant (rs378147396). Indeed, a variety of DNA variant annotations, such as downstream variants, upstream variants, intronic variants, and splice region variants, within the *KALRN* gene were significantly associated with MAP in the present study.

In total, we identified 22 positional candidate genes within the 47 QTL associated with MAP (Table 3), of which 10 were identified as potential functional candidate genes. Upon investigating the literature for potential biological functions of each, the most likely functional candidate genes identified along with *KALRN*, are zinc finger and BTB domain containing 20 (*ZBTB20*), lipoma-preferred partner (*LPP*), src-like-adapter 2 (*SLA2*), coagulation factor XIII A chain (*F13A1*), leucine-rich repeats and calponin homology (*CH*) domain containing 3 (*LRCH3*), DnaJ heat shock protein family (*Hsp40*) Member C6 (*DNAJC6*), zinc finger *DHHC*-type containing 14 (*ZDHHC14*), sorting nexin-1 (*SNX1*), and hyaluronan synthase 2 (*HAS2*).

Seventy-six distinct bovine biological pathways were initially identified using the list of 623 positional candidate genes. After applying the hypergeometric algorithm, 29 pathways had an unadjusted *P*-value <0.05 (Supplemental Table S2; https://doi.org/10.3168/jds.2018-15906). After applying the Benjamini-Hochberg correction, none of the pathways were identified as being enriched (minimum corrected *P*-value = 0.108). When known data on human biological pathways were included in the pathway analyses, 482 orthologous biological pathways were identified. Of these, 64 pathways had an unadjusted *P*-value <0.05 (Supplemental Table S3; https://doi.org/10.3168/jds.2018-15906). Once the Benjamini-Hochberg adjustment was applied, none of the pathways were identified as being enriched (minimum corrected *P*-value = 0.239).

DISCUSSION

The challenges in addressing many cattle diseases, including bovine paratuberculosis, necessitates consideration of other disease mitigation strategies, one of which could be animal breeding. One of the advantages of breeding as a strategy to improve animal health is that it is cumulative and permanent, with the genetic merit of a given animal being a function of all selection decisions made throughout its ancestral generations. Because the female must become pregnant to initiate a subsequent lactation, the marginal cost incurred to use superior germplasm semen is usually minimal. Given the detected existence of substantial genetic variation in humoral response to MAP in the present study, the justification for considering genetic merit for humoral response to MAP in a breeding program is therefore strong. This was substantiated by the exercise in the present study that validated MAP EBV, where a 1.43 greater odds of yielding a positive MAP result was detected in cows ranked poorly on genetic merit for

Table 3. Quantitative trait loci (QTL) identified as being associated with humoral response to *Mycobacterium avium* subspecies *paratuberculosis*[1]

BTA	QTL start (bp)	QTL end (bp)	*P*-value for most significant SNP	Favorable allele	Favorable allele frequency	Allele substitution effect	Significant SNP position	Annotation	Candidate gene	No. of genes in QTL	No. of significant SNP in QTL
1	26,167,312	26,446,316	4.129×10^{-8}	C	0.005	0.007	26,279,218	Intergenic		1	1
1	28,407,185	28,494,094	1.483×10^{-8}	C	0.007	0.006	28,407,185	Upstream	*ENSBTAG00000005101*	1	1
1	59,604,462	59,612,006	1.124×10^{-9}	G	0.006	0.008	59,612,006	Intron	*ZBTB20*	1	1
1	64,369,225	69,754,155	2.137×10^{-13}	C	0.006	0.009	69,624,778	Intron	*KALRN*	60	51
1	69,764,180	69,764,180	3.433×10^{-9}	T	0.012	0.005	69,764,180	Intron	*UMPS*	1	1
1	70,108,608	71,811,570	3.611×10^{-9}	G	0.007	0.006	70,854,219	Intron	*LRCH3*	27	65
1	79,588,937	79,588,937	1.723×10^{-9}	A	0.006	0.011	79,588,937	Intron	*LPP*	1	1
1	80,447,980	80,447,980	3.651×10^{-8}	C	0.007	0.005	80,447,980	Intergenic	—	—	1
1	88,842,592	88,847,970	1.679×10^{-9}	G	0.006	0.010	88,842,592	Intergenic	—	—	3
1	112,715,335	119,581,742	5.777×10^{-12}	A	0.006	0.012	113,546,452	Intergenic	—	40	10
3	4,670,952	4,670,966	1.735×10^{-9}	T	0.006	0.010	4,670,952	Intergenic	—	—	3
3	79,626,954	80,275,067	1.814×10^{-8}	A	0.003	0.997	80,275,067	Intron	*DNAJC6*	5	2
5	96,254,052	99,194,836	7.170×10^{-10}	A	0.008	0.006	98,598,926	Intergenic		28	2
6	55,845,383	55,845,383	2.589×10^{-8}	A	0.007	0.006	55,845,383	Intergenic	—	—	1
8	81,381,959	81,857,714	4.294×10^{-8}	G	0.005	0.010	81,782,508	Intergenic		2	2
9	73,680,357	73,821,094	1.557×10^{-8}	T	0.005	0.012	73,726,695	Intergenic	—	—	1
9	87,476,619	90,634,355	7.548×10^{-13}	C	0.005	0.021	89,425,331	Intergenic		27	2
9	91,561,782	91,571,541	4.495×10^{-9}	T	0.006	0.012	91,571,541	Intergenic	—	—	1
9	92,215,914	92,215,914	1.531×10^{-8}	G	0.007	0.005	92,215,914	Intergenic		—	1
9	95,503,522	95,897,049	6.589×10^{-13}	C	0.010	0.005	95,619,684	Intron	*ZDHHC14*	3	2
10	44,616,944	48,347,572	3.683×10^{-8}	G	0.006	0.010	45,898,484	Downstream	*SNX1*	35	1
11	5,908,958	5,908,958	1.915×10^{-10}	A	0.007	0.006	5,908,958	Intron	*NPAS2*	1	1
11	6,005,215	6,005,215	8.296×10^{-11}	C	0.008	0.005	6,005,215	Downstream	*NPAS2*	1	1
11	6,150,881	6,150,890	8.777×10^{-11}	T	0.008	0.005	6,150,881	Intergenic		—	2
11	6,187,500	6,241,603	1.568×10^{-11}	A	0.004	0.017	6,227,418	Intron	*RNF149*	2	1
11	6,327,860	6,327,860	4.972×10^{-8}	G	0.006	0.007	6,327,860	Intron	*RFX8*	1	1
11	6,333,224	6,333,267	1.807×10^{-8}	G	0.003	0.030	6,333,255	Intron	*RFX8*	1	2
11	9,606,899	9,606,899	1.246×10^{-8}	A	0.003	0.030	9,606,899	Intron	*TACR1*	1	1
13	28,234,519	30,909,480	1.338×10^{-8}	A	−0.007	0.005	29,951,397	Intergenic		19	1
13	62,037,755	62,037,755	1.942×10^{-9}	C	0.007	0.006	62,037,755	Intron	*XKR7*	1	1
13	66,373,805	66,373,805	6.292×10^{-10}	T	0.006	0.008	66,373,805	Intron	*SLA2*	1	1
13	70,488,028	72,329,336	2.910×10^{-8}	A	0.003	0.027	72,023,756	Intergenic		12	1
14	16,944,837	21,128,294	2.276×10^{-8}	A	0.006	0.008	19,711,487	Intron	*HAS2*	32	1
14	33,563,774	33,601,252	3.990×10^{-8}	T	−0.001	0.297	33,588,051	Intron	*CPA6*	1	1
18	50,390,456	52,265,553	2.677×10^{-11}	G	0.007	0.009	51,899,478	Intron	*TEX101*	58	28
18	53,905,719	61,291,660	3.048×10^{-11}	A	0.009	0.005	61,212,502	Intron	*ENSBTAG00000040392*	243	7
21	62,644,820	62,644,820	1.414×10^{-8}	G	0.005	0.013	62,644,820	Intergenic	—	—	1
23	46,741,649	46,741,649	3.792×10^{-8}	A	0.003	0.040	46,741,649	Intergenic	—	—	1
23	48,411,393	48,482,001	3.669×10^{-8}	T	0.006	0.009	48,460,057	Intergenic		1	1
23	48,741,897	48,741,897	5.799×10^{-9}	T	0.007	0.006	48,741,897	Intron	*F13A1*	1	1
23	49,577,226	49,659,683	2.135×10^{-8}	T	0.006	0.009	49,577,226	Intron	*CDYL*	1	1
25	5,454,814	5,454,814	9.015×10^{-9}	T	0.006	0.012	5,454,814	Intergenic		—	1
25	32,829,869	32,829,869	1.277×10^{-9}	T	0.004	0.024	32,829,869	Intergenic		—	1
26	7,959,610	7,959,610	3.889×10^{-9}	C	0.005	0.012	7,959,610	Intron	*PRKG1*	1	1
27	6,246,011	6,544,550	1.185×10^{-8}	A	0.004	0.018	6,544,550	Intergenic		2	1
29	31,234,645	31,234,645	1.608×10^{-8}	T	0.006	0.008	31,234,645	Intergenic			1
29	32,448,786	34,312,188	4.508×10^{-11}	G	0.006	0.009	33,280,610	Intergenic		11	10

[1]Note, for cases where >1 SNP possessed the same *P*-value but was associated with the same positional candidate gene, the first (position-wise) SNP was reported. MAF = minor allele frequency of the favorable allele.

MAP relative to their herd contemporaries ranked best on genetic merit for MAP. Twomey et al. (2016) undertook a similar EBV validation exercise based on cows divergent in parental average EBV for liver fluke. The area reported under the receiver operating curver reported by Twomey et al. (2016) was 0.522, with cows in the top (i.e., worst) 10% being 1.28 (95% CI = 1.05–1.36) times more likely to have livers damaged by liver fluke compared with contemporaries in the bottom (i.e., best) 10%. This difference in odds translated to a 6% unit probability difference between the top and bottom 10% of cows in the study cohort. Similarly, using bovine tuberculosis (**bTB**) infection data in cattle, Ring et al. (2019) reported a mean prevalence of 9.3% in cows in the worst 20% on parental EBV for bTB versus a mean prevalence of 6.9% in cows in the best 20% on parental EBV for bTB; this equated to an odds ratio of 1.44. The area under the receiver operating curve reported was 0.529 (95% CI = 0.5236–0.5342) for the present study. These 2 validation studies, together with the results from the validation exercise in present study, clearly demonstrate the potential health gains achievable with genetic selection. Whereas the mean EBV reliability of the validation cows in the present study was low (i.e., on average 0.145), further ability to differentiate could have been achieved if the reliability of the EBV was greater. Such an increase in reliability could be achieved through access to more phenotypic data or the inclusion of genomic information in the prediction process (Meuwissen et al., 2001). Using the approach proposed by Wray et al. (2010), assuming a heritability of humoral response to MAP of 0.05 and a prevalence of 7.7%, the area under the receiver operating curve to predict the outcome for humoral response to MAP would increase from 0.56 if only a quarter of the genetic variance in the phenotype could be explained; the area would increase to 0.59 and eventually to 0.63 if half and all of the genetic variance could be explained, respectively.

A key question to be addressed in future studies is whether selecting for or against positive antibody response to MAP is beneficial for cattle populations. It could be surmised that selecting against positive antibody response is, in reality, selecting for the animals that can maintain a degree of internal cellular homeostasis despite having been infected by MAP. Such animals may in fact be shedding MAP, yet may not progress to the advanced clinical stages of bovine paratuberculosis. Irrespective, single trait selection for any trait is never recommended; thus, any consideration of breeding for changes in the antibody response to MAP should be undertaken within the framework of a multitrait breeding objective.

Estimated Variance Components for MAP in Comparison to Previous Studies

Previous studies that estimated genetic parameters for paratuberculosis in cattle suggest heritability estimates of susceptibility to the disease range from <0.01 (Koets et al., 1999) to 0.283 (Küpper et al., 2012); all studies to-date (which reported the actual breed of cattle used) have been undertaken in dairy cattle. A meta-analysis of the 2 available studies (Hinger et al., 2008; Berry et al., 2010) on dichotomized humoral response to MAP using blood ELISA and linear animal models, similar to the strategy adopted in the present study, resulted in a pooled heritability estimate of 0.072 (pooled SE = 0.014); this was not different from the 0.05 (SE = 0.008) estimated in the present study. Once the prevalence of the previous estimates of heritability for dichotomized humoral response to MAP using ELISA were adjusted to a prevalence of 7.7%, as observed in the present study, the heritability on the underlying scale (Robertson and Lerner, 1949) varied from 0.19 (Hinger et al., 2008) to 0.34 (Berry et al., 2010), with an overall mean pooled heritability estimate of 0.234 for the 2 studies; the corresponding value for the present study was 0.17. Neither the additive genetic standard deviation nor the residual standard deviation for the dichotomized humoral response to MAP were reported by Hinger et al. (2008) or Berry et al. (2010). As such, the additive genetic standard deviation and residual standard deviation in dichotomized humoral response to MAP infection reported in the present study cannot be compared.

The heritability estimate for the humoral response to MAP infection using a sire model and the 33,818 cows in herds with at least 5 positive cows and at least 1 of those cows yielding a positive ELISA to MAP in the present study was of a similar magnitude as that reported by Kirkpatrick and Lett (2018). The range reported by Kirkpatrick and Lett (2018) using sire models and dichotomized humoral (or milk) antibody response to MAP was 0.041 (SE = 0.004) to 0.062 (SE = 0.007). The upper and lower limits of this range were based on cohorts of herds with at least 1 positive test (n = 999 sires represented by 222,872 daughter ELISA records) and ≥5% positive tests (n = 475 sires represented by 65,289 daughter ELISA records), respectively. Perhaps, as suggested by Kirkpatrick and Lett (2018), a sire threshold model analysis is a better analysis to conduct to gain an accurate estimate of the true heritability value for antibody responses to MAP infection. This approach may ameliorate the effects of the prevalence of MAP on a per-cohort basis on the estimates of heritability for dichotomized humoral response to MAP

infection. When the heritability estimates for dichotomized antibody response to MAP using blood or milk ELISA were adjusted to the prevalence reported in the present study (7.7%), the heritability on the underlying scale (Robertson and Lerner, 1949) varied from 0.14 to 0.21; the corresponding value for the present study was 0.16.

The additive genetic standard deviation for humoral response to MAP was reported only by Gao et al. (2018) and was 0.125, which is considerably higher than the genetic standard deviation of 0.058 in the present study. The residual standard deviation [again, only reported by Gao et al. (2018)] was 0.55, compared with the lower estimate of 0.25 reported in the present study. Hence, the lower heritability reported in the present study could be attributed to a relatively larger residual variance and lower genetic variance compared with other studies. Compounding this could be the fact that heritability estimate ranges reported in the present study on a per laboratory basis demonstrate site-specific levels of noise (i.e., residual variance). Noise could have been introduced in part due to environmental differences that existed between the laboratories (e.g., laboratory technicians at each laboratory could have possessed various levels of experience in conducting ELISA). Furthermore, these assays may have been a routine procedure in some laboratories that specialize in such assays, but an infrequent assay conducted in others. These factors, among others may have contributed to varying levels of residual variance being introduced on a per laboratory basis. Moreover, the somewhat low heritability estimate could also be attributed to the imperfect nature of ELISA tests in diagnosing cases and controls. As ELISA rely on the humoral response of individuals, they may not detect animals that are in the early stages of MAP infection, as they may not have mounted a humoral response to MAP infection at the point of testing (and may not for months, or even years). This results in infected animals being reported as ELISA negative to MAP despite shedding MAP into the environment (Milner et al., 1987). False-positive humoral results can also arise due to bTB-infected animals, and bTB testing in herds before MAP testing without sufficient time elapsing between tests (i.e., 90 d; Lilenbaum et al., 2007; Varges et al., 2009). Environmental mycobacteria (closely related to, but excluding MAP) could also potentially result in false-positive ELISA results in the present study (Osterstock et al., 2007). As such, this misclassification introduces noise, thus biasing down heritability estimates (Milner et al., 1987; Bishop and Woolliams, 2010).

Despite the relatively low heritability for humoral response to MAP in the present study, an accuracy of selection of 0.34 could be achieved with phenotypic information on just 10 progeny. Similarly, based solely on progeny phenotypes in a univariate genetic evaluation, MAP phenotypes on just 76 progeny would be required to achieve an accuracy of selection for humoral response to MAP of 0.70. High accuracy of selection is thus achievable in the presence of a national recording system for humoral response to MAP in cattle.

Candidate Genes Associated with Humoral Response to MAP

Of the 22 positional candidate genes identified in the 47 identified QTL, 10 were identified as potential functional candidate genes based upon their gene ontology results and previous reports on their function in the literature (Bannantine and Bermudez, 2013; Liu et al., 2013; Marton et al., 2015). Some of these genes are novel in the sense that they have not previously been associated with bovine paratuberculosis. The functional candidate genes of interest identified were *KALRN*, *ZBTB20*, *LPP*, *SLA2*, *F13A1*, *LRCH3*, *DNAJC6*, *ZGHHC14*, *SNX1*, and *HAS2*; the (potential) biological functions of these are outlined below. All candidate genes have been shown to exhibit an expression profile in the bovine colon, duodenum, ileum, spleen, and lymph nodes (Harhay et al., 2010). As stated by Brito et al. (2018), resistance or susceptibility to MAP infection appears to be a highly polygenic trait, reflecting the nature of bovine paratuberculosis, which is, indeed, a highly complex trait. As such, the environmental influence on the manifestation of the trait must not be ignored. This influence may in part give rise to the fact that previous studies have implicated all *Bos taurus* autosomes as having an association with bovine paratuberculosis, yet little consistency has been observed among the reported genomic locations of these studies. Other factors that must be considered as contributors to this lack of coherence include the low heritability of the trait, inconsistent methods to classify MAP-positive or -negative animals, and divergent statistical methodologies employed on varying sample sizes of different cattle populations (Brito et al., 2018). Specific to the present study, another factor contributing to spurious results is the error in genotype imputation from sequence data. Despite the methods employed in the present study yielding a high imputation accuracy of 98%, the 2% error may have affected the allele frequencies of the population, and thus the significance of some of the SNP associations obtained. Nevertheless, the results of the present study corroborate some previous findings in cattle, whereas some results agree with those identified in human populations.

KALRN. Gene ontology results for *KALRN*, found in a QTL on BTA1 (between positions 64369225 and

69754155), support it as a strong candidate gene influencing humoral response to MAP infection because of its role in encoding for the RhoGEF kinase protein. Human tissues, such as the duodenum, colon, lymph nodes, small intestine, and spleen, have been reported to have expressed *KALRN* (Fagerberg et al., 2014), all of which are important in the pathology of Johne's disease. Biological processes in which the RhoGEF kinase protein is involved include the positive regulation of Rho protein signal transduction as well as positive regulation of Rho GTPase activity. This is particularly interesting considering that the RhoA GTPase protein is located in intestinal epithelial cells and, upon stimulation by MAP, the bacteria infiltrates the intestinal submucosa (Bannantine and Bermudez, 2013). Infiltration of, and transcytosis through, the intestinal submucosa is crucial for MAP growth and replication, as it facilitates the bacterium crossing from the intestinal lumen to its target cells (i.e., macrophage and dendritic cells). From within macrophage and dendritic cells, MAP successfully modulates the host's immune responses, subverting immune attack. The intracellular subversion enables the bacterium to establish a niche within the host, providing it sufficient time to grow, replicate, and spread through the surrounding intestines and lymph nodes (Bannantine and Bermudez, 2013; Arsenault et al., 2014; Koets et al., 2015). Furthermore, the rho kinase signal pathway has previously been implicated in inflammatory bowel disease (**IBD**) in humans, playing roles in intestinal barrier damage, abnormal immune response, and intestinal fibrosis (Huang et al., 2015). Brito et al. (2018) also identified *KALRN* as a candidate gene in an independent population of ELISA-tested Canadian Holstein cattle. Thus, it is not unrealistic to hypothesize that *KALRN* plays an important role in the aforementioned processes in cattle susceptible to Johne's disease.

ZBTB20. Gene ontology results implicate the gene's product in metal ion binding processes. The fact that MAP cannot endogenously produce mycobactin (necessary for iron transport) makes it an obligate intracellular parasite dependent upon the host for iron uptake and metabolism (Clark et al., 2008; McNees et al., 2015; Rathnaiah et al., 2017). Perhaps while subverting the host immune system inside target cells, MAP uses *ZTBT20* to provide it with a means of exogenous iron to grow and replicate. The *ZTBT20* gene has also been implicated in promoting Toll-like receptor-triggered innate immune responses in hosts via repressing the transcription of *IKBA*, which in turn promotes the activation of *NFKB* (Liu et al., 2013). This corroborates the results of the gene set enrichment analysis conducted by Kiser et al. (2017) in cattle, where enrichment analyses identified pathways involved with *NFKB*. Toll-like receptors have also been previously implicated in bovine paratuberculosis through candidate gene studies (Mucha et al., 2009; Koets et al., 2015). Expression of *ZBTB20* has been observed in human tissues relevant to Johne's disease, such as the colon, duodenum, lymph nodes, small intestine, and spleen (Fagerberg et al., 2014). Moreover, *ZBTB20* was also identified as a candidate gene in the genome-wide association study conducted by Brito et al. (2018) in dairy cows, further substantiating the evidence that *ZBTB20* could indeed be associated with the resistance status of cattle to MAP.

LPP. The potential role for *LPP* in the etiology of Johne's disease could lie in the fact that it aids in signal transduction, cell migration, cytoskeletal remodeling, and cell-cell adhesion (Jin et al., 2009). Although its exact function has yet to be established, *LPP* has been shown to enhance cell migration in response to cellular injury and has been linked to diseases such as atherosclerosis, a disorder characterized by an excessive chronic inflammatory immune response. Initially, this acute inflammatory response is beneficial in protecting the host during immune challenges, but it becomes detrimental to the host when it turns chronic in nature (Ross and Agius, 1992). The chronicity of the inflammatory response causes the disease due to the fibroproliferative properties of the response resulting in granulomatous tissue (Ross and Agius, 1992; Kunkel et al., 1998). Perhaps what is an initial beneficial host immune response to MAP infection, progresses to become a chronic malignant overactivation of the host immune response. Coordinated in part by *LPP*, this response could result in the chronic granulomatous gastroenteritis characteristic of Johne's disease. It could also be surmised that MAP uses *LPP* to intracellularly modulate macrophage lipoprotein metabolism for the benefit of the bacteria, whereas the recruitment of macrophages to the intestinal epithelium would maximize the bacteria's opportunity to infiltrate host cells that enable it to grow and replicate. Human tissue expression studies report that *LPP* is expressed in the colon, duodenum, lymph nodes, small intestine, and spleen (Fagerberg et al., 2014).

SLA2. Gene ontology results for *SLA2* includes T cell activation, which is an integral part of the host immune response. The src-like adaptor protein 2 (**SLAP-2**), encoded by *SLA2*, has been observed to be expressed in the small intestine, colon, spleen, and lymph nodes in humans (Fagerberg et al., 2014). As reviewed by Marton et al. (2015), SLAP-2 negatively regulates the antigen receptor signaling action of both B and T lymphocytes, thus suppressing host immune responses. It has also been suggested that SLAP-2 is necessary for the maturation and activation of mono-

cyte and dendritic cells (Liontos et al., 2011). Perhaps MAP modulates the expression of *SLA2* within monocytes, thus subverting the host immune responses long enough for sufficient growth and replication to thrive.

F13A1. Encoding for coagulation factor XIIIA, *F13A1* is a strong candidate gene in the etiology of Johne's disease, as it promotes wound healing in damaged tissues, providing structural support and repaired vascularization. Coagulation factor XIIIA has also been implicated in IBD, as, similar to atherogenesis, these initial beneficial mechanisms can in fact become detrimental to the host. The chronic inflammation observed in humans suffering from IBD is characterized by a hypercoagulable state accompanied by aberrations in coagulation processes (Danese et al., 2007). Mechanisms coordinated by coagulation factor XIII can cause increased neovascularization and impaired mucosal healing, which can cause additional inflammation in patients suffering from IBD (Gemmati et al., 2016). Genetic variation in *F13A1* could result in susceptibility to Johne's disease through abnormal coagulation processes. The human colon, duodenum, lymph node, small intestine, and spleen express *F13A1* (Fagerberg et al., 2014).

LRCH3. Although there is a relative paucity of information in the literature regarding this gene, members of the leucine-rich repeat family are thought to be critical in initiating inflammatory innate immune responses (Bell et al., 2003). Specifically, *LRCH3*, which is a member of this family, is a potential candidate gene involved in the pathology of Johne's disease, as it has previously been implicated in nuclear factor-κB activation mechanisms in the nuclear factor-κB immunoregulatory pathways (Gewurz et al., 2012). This evidence corroborates the aforementioned evidence of the gene set enrichment analysis conducted by Kiser et al. (2017). Moreover, evidence in the literature has shown that *LRCH3* is significantly differentially expressed between healthy colorectal tissue sample controls and samples presenting with colorectal cancer; the cancerous tissue samples exhibited a higher level of *LRCH3* expression (Piepoli et al., 2012).

DNAJC6. The *DNAJC6* has been shown to be a useful biomarker in the design of predictive algorithms that classify the severity of IBD in patients to better diagnose and improve patient quality of life (Montero-Meléndez et al., 2013). Also known as *PARK19*, *DNAJC6* has also been implicated in Parkinson's disease (Ran and Belin, 2014). Following a review of the available literature, Dow (2014) hypothesized that there could indeed be a link between MAP and Parkinson's disease in humans, a hypothesis which is yet to be confirmed.

ZDHHC14. Zinc finger DHHC domain-containing 14 protein has been shown by Oo et al. (2014) to promote migration and invasion of scirrhous-type gastric cancer, promoting tumor progression when overexpressed. The overexpression of this gene was significantly associated with scirrhous patterning and the degree of the depth of cancer tumor invasion of gastric mucosa tissue collected from patients suffering from gastric cancer. As such, it is not unreasonable to hypothesize that *ZDHHC14* plays a role in Johne's disease, considering it is also a chronic, progressive disease of the gastrointestinal tract.

SNX1. Downregulation of *SNX1* has been linked to drug resistance in colorectal cancer as well as predicting poor prognosis for the disease (Bian et al., 2016). Specifically, the downregulation of *SNX1* has been strongly associated with poor overall survival rate of patients suffering from colorectal cancer. Bian et al. (2016) hypothesized that upregulation of the gene could provide a novel therapeutic intervention for this disease, an approach which could potentially be translated to veterinary medicine for the treatment of Johne's disease in the future. Interestingly, synergy may exist between the susceptible alleles for the *KALRN* gene and the susceptible alleles for the *SNX1* gene, as Prosser et al. (2010) have shown that *SNX1* interacts with the Rac1 and RhoG guanine nucleotide exchange factor Kalirin-7. This process recruits the inactive Rho GTPase to its exchange factor, influencing cell membrane remodeling, which is perhaps a similar interaction as occurs to initiate the process outlined above.

HAS2. Upregulation of *HAS2*, which produces hyaluronan synthesis, has been shown to be associated with IBD (among other inflammatory diseases) and has been shown to be expressed in human intestinal cells under the influence of the proinflammatory cytokine IL-1β (Ducale et al., 2005). In fact, Vigetti et al. (2010) demonstrated that, in endothelial cells, monocyte adhesion depends strongly on hyaluronan. Throughout the inflammatory response, cells produce hyaluronan matrices, which in turn promote the adhesion of monocytes and macrophages to cell surfaces. This aids in the processes governing the transformation of macrophages into foam cells, which contributes toward atherosclerotic plaque formations, very similar to *F13A1* outlined above. Vigetti et al. (2010) also demonstrated that IL-1β, and tumor necrosis factors-α and -β strongly induce hyaluronan synthesis via the *NFKB* pathway, which, again, was previously implicated in the pathology of Johne's disease by Kiser et al. (2017).

CONCLUSIONS

Exploitable genetic variation in humoral response to MAP exists in the Holstein-Friesian population sampled in the present study. Thus, ample opportunity exists to capitalize on this variation through a breeding

program for reduced MAP susceptibility. Moreover, the biological insights achieved from the identified QTL and candidate genes provide novel evidence to support the notion that bovine paratuberculosis is molecularly similar to IBD in humans; validation of the results reported herein are, nonetheless, crucial especially for the low-minor allele frequency SNP. Candidate genes and QTL regions reported within could also be used a priori in any further analyses, either association studies or genomic or phenotypic predictions that exploit Bayesian techniques. Furthermore, the results from the present study potentially enable researchers to gain a greater understanding of bovine paratuberculosis and potential therapeutic targets for future investigation, as breakthroughs in the treatment for IBD may also be transferable to veterinary medicine.

ACKNOWLEDGMENTS

Funding from the Irish Department of Agriculture, Food and the Marine Stimulus research grant HealthyGenes (Dublin) and Science Foundation Ireland (SFI, Dublin) principal investigator award grant number 14/IA/2576 is greatly appreciated as is the support from a research grant from both Science Foundation Ireland and the Department of Agriculture, Food and Marine on behalf of the Government of Ireland under the Grant 16/RC/3835 (VistaMilk). We gratefully acknowledge the 1000 Bull Genomes Consortium (Melbourne, Australia) for providing accessibility to whole-genome sequence data which was used in this study.

REFERENCES

Alpay, F., Y. Zare, M. H. Kamalludin, X. Huang, X. Shi, G. E. Shook, M. T. Collins, and B. W. Kirkpatrick. 2014. Genome-wide association study of susceptibility to infection by *Mycobacterium avium* subspecies *paratuberculosis* in Holstein cattle. PLoS One 9:e111704.

Arsenault, R. J., P. Maattanen, J. Daigle, A. Potter, P. Griebel, and S. Napper. 2014. From mouth to macrophage: mechanisms of innate immune subversion by *Mycobacterium avium* ssp. *paratuberculosis*. Vet. Res. 45:54.

Bannantine, J. P., and J. E. Bermudez. 2013. No holes barred: Invasion of the intestinal mucosa by *Mycobacterium avium* ssp. *paratuberculosis*. Infect. Immun. 81:3960–3965.

Beissinger, T. M., G. J. Rosa, S. M. Kaeppler, D. Gianola, and N. De Leon. 2015. Defining window-boundaries for genomic analyses using smoothing spline techniques. Genet. Sel. Evol. 47:30.

Bell, J. K., G. E. Mullen, C. A. Leifer, A. Mazzoni, D. R. Davies, and D. M. Segal. 2003. Leucine-rich repeats and pathogen recognition in Toll-like receptors. Trends Immunol. 24:528–533.

Berry, D. P., and R. D. Evans. 2014. Genetics of reproductive performance in seasonal calving beef cows and its association with performance traits. J. Anim. Sci. 92:1412–1422.

Berry, D. P., M. Good, P. Mullowney, A. R. Cromie, and S. J. More. 2010. Genetic variation in serological response to *Mycobacterium avium* subspecies *paratuberculosis* and its association with performance in Irish Holstein-Frieisian dairy cows. Livest. Sci. 131:102–107.

Bian, Z., Y. Feng, Y. Xue, Y. Hu, Q. Wang, L. Zhou, Z. Liu, J. Zhang, Y. Yin, B. Gu, and Z. Huang. 2016. Down-regulation of SNX1 predicts poor prognosis and contributes to drug resistance in colorectal cancer. Tumour Biol. 37:6619–6625. https://doi.org/10.1007/s13277-015-3814-3.

Bishop, S. C., and J. A. Woolliams. 2010. On the genetic interpretation of disease data. PLoS One 5:e8940.

Breuer, K., A. K. Foroushani, M. R. Laird, C. Chen, A. Sribnaia, R. Lo, G. L. Winsor, R. E. Hancock, F. S. Brinkman, and D. J. Lynn. 2013. InnateDB: Systems biology of innate immunity and beyond–recent updates and continuing curation. Nucleic Acids Res. 41:D1228–D1233.

Brito, L. F., S. Mallikarjunappa, M. Sargolzaei, A. Koeck, J. Chesnais, F. S. Schenkel, K. G. Meade, F. Miglior, and N. A. Karrow. 2018. The genetic architecture of milk ELISA scores as an indicator of Johne's disease (paratuberculosis) in dairy cattle. J. Dairy Sci. 101:10062–10075.

Browning, B. L., and S. R. Browning. 2016. Genotype imputation with millions of reference samples. Am. J. Hum. Genet. 98:116–126.

Clark, D. L., Jr., J. J. Koziczkowski, R. P. Radcliff, R. A. Carlson, and J. L. Ellingson. 2008. Detection of *Mycobacterium avium* subspecies *paratuberculosis*: Comparing fecal culture versus serum enzyme-linked immunosorbent assay and direct fecal polymerase chain reaction. J. Dairy Sci. 91:2620–2627.

Collins, M. T. 2003. Paratuberculosis: Review of present knowledge. Acta Vet. Scand. 44:217–221.

Daetwyler, H. D., A. Capitan, H. Pausch, P. Stothard, R. Van Binsbergen, R. F. Brondum, X. P. Liao, A. Djari, S. C. Rodriguez, C. Grohs, D. Esquerre, O. Bouchez, M. N. Rossignol, C. Klopp, D. Rocha, S. Fritz, A. Eggen, P. J. Bowman, D. Coote, A. J. Chamberlain, C. Anderson, C. P. VanTassell, I. Hulsegge, M. E. Goddard, B. Guldbrandtsen, M. S. Lund, R. F. Veerkamp, D. A. Boichard, R. Fries, and B. J. Hayes. 2014. Whole-genome sequencing of 234 bulls facilitates mapping of monogenic and complex traits in cattle. Nat. Genet. 46:858–865.

Danese, S., A. Papa, S. Saibeni, A. Repici, A. Malesci, and M. Vecchi. 2007. Inflammation and coagulation in inflammatory bowel disease: The clot thickens. Am. J. Gastroenterol. 102:174–186.

Das, S., L. Forer, S. Schonherr, C. Sidore, A. E. Locke, A. Kwong, S. I. Vrieze, E. Y. Chew, S. Levy, M. McGue, D. Schlessinger, D. Stambolian, P. R. Loh, W. G. Iacono, A. Swaroop, L. J. Scott, F. Cucca, F. Kronenberg, M. Boehnke, G. R. Abecasis, and C. Fuchsberger. 2016. Next-generation genotype imputation service and methods. Nat. Genet. 48:1284–1287.

Del Corvo, M., M. Luini, A. Stella, G. Pagnacco, P. Ajmone-Marsan, J. L. Williams, and G. Minozzi. 2017. Identification of additional loci associated with antibody response to *Mycobacterium avium* ssp *paratuberculosis* in cattle by GSEA-SNP analysis. Mamm. Genome 28:520–527.

Dow, C. T. 2014. M. paratuberculosis and Parkinson's disease—Is this a trigger. Med. Hypotheses 83:709–712. https://doi.org/10.1016/j.mehy.2014.09.025.

Ducale, A. E., S. I. Ward, T. Dechert, and D. R. Yager. 2005. Regulation of hyaluronan synthase-2 expression in human intestinal mesenchymal cells: mechanisms of interleukin-1beta-mediated induction. Am. J. Physiol. Gastrointest. Liver Physiol. 289:G462–G470.

Fabregat, A., S. Jupe, L. Matthews, K. Sidiropoulos, M. Gillespie, P. Garapati, R. Haw, B. Jassal, F. Korninger, B. May, M. Milacic, C. D. Roca, K. Rothfels, C. Sevilla, V. Shamovsky, S. Shorser, T. Varusai, G. Viteri, J. Weiser, G. Wu, L. Stein, H. Hermjakob, and P. D'Eustachio. 2018. The reactome pathway knowledgebase. Nucleic Acids Res. 46:D649–D655.

Fagerberg, L., B. M. Hallstrom, P. Oksvold, C. Kampf, D. Djureinovic, J. Odeberg, M. Habuka, S. Tahmasebpoor, A. Danielsson, K. Edlund, A. Asplund, E. Sjostedt, E. Lundberg, C. A. Szigyarto, M. Skogs, J. O. Takanen, H. Berling, H. Tegel, J. Mulder, P. Nilsson, J. M. Schwenk, C. Lindskog, F. Danielsson, A. Mardinoglu, A. Sivertsson, K. von Feilitzen, M. Forsberg, M. Zwahlen, I. Olsson, S. Navani, M. Huss, J. Nielsen, F. Ponten, and M. Uhlen. 2014. Analysis of the human tissue-specific expression by genome-wide

integration of transcriptomics and antibody-based proteomics. Mol. Cell. Proteomics 13:397–406.
Gao, Y., J. Cao, S. Zhang, Q. Zhang, and D. Sun. 2018. Short communication: Heritability estimates for susceptibility to *Mycobacterium avium* ssp *paratuberculosis* infection in Chinese Holstein cattle. J. Dairy Sci. 101:7274–7279.
Garrick, D. J., J. F. Taylor, and R. L. Fernando. 2009. Deregressing estimated breeding values and weighting information for genomic regression analyses. Genet. Sel. Evol. 41:55. https://doi.org/10.1186/1297-9686-41-55.
Gemmati, D., M. Vigliano, F. Burini, R. Mari, H. H. El Mohsein, F. Parmeggiani, and M. L. Serino. 2016. Coagulation Factor XIIIA (F13A1): Novel perspectives in treatment and pharmacogenetics. Curr. Pharm. Des. 22:1449–1459.
Geraghty, T., D. A. Graham, P. Mullowney, and S. J. More. 2014. A review of bovine Johne's disease control activities in 6 endemically infected countries. Prev. Vet. Med. 116:1–11. https://doi.org/10.1016/j.prevetmed.2014.06.003.
Gewurz, B. E., F. Towfic, J. C. Mar, N. P. Shinners, K. Takasaki, B. Zhao, E. D. Cahir-McFarland, J. Quackenbush, R. J. Xavier, and E. Kieff. 2012. Genome-wide siRNA screen for mediators of NF-κB activation. Proc. Natl. Acad. Sci. USA 109:2467–2472. https://doi.org/10.1073/pnas.1120542109.
Gilmour, A. R., B. J. Gogel, B. R. Cullis, and R. Thompson. (2009). ASReml User Guide Release 3.0. VSN International Ltd., Hemel Hempstead, UK.
Harhay, G. P., T. P. Smith, L. J. Alexander, C. D. Haudenschild, J. W. Keele, L. K. Matukumalli, S. G. Schroeder, C. P. Van Tassell, C. R. Gresham, S. M. Bridges, S. C. Burgess, and T. S. Sonstegard. 2010. An atlas of bovine gene expression reveals novel distinctive tissue characteristics and evidence for improving genome annotation. Genome Biol. 11:R102.
Harris, N. B., and R. G. Barletta. 2001. *Mycobacterium avium* ssp. *paratuberculosis* in veterinary medicine. Clin. Microbiol. Rev. 14:489–512. https://doi.org/10.1128/CMR.14.3.489-512.2001.
Hinger, M., H. Brandt, and G. Erhardt. 2008. Heritability estimates for antibody response to Mycobacterium avium subspecies paratuberculosis in German Holstein cattle. J. Dairy Sci. 91:3237–3244.
Huang, Y., S. Y. Xiao, and Q. H. Jiang. 2015. Role of Rho kinase signal pathway in inflammatory bowel disease. Int. J. Clin. Exp. Med. 8:3089–3097.
Jin, L., N. E. Hastings, B. R. Blackman, and A. V. Somlyo. 2009. Mechanical properties of the extracellular matrix alter expression of smooth muscle protein LPP and its partner palladin; relationship to early atherosclerosis and vascular injury. J. Muscle Res. Cell Motil. 30:41–55.
Johne, H. A., and L. Frothingham. 1895. Ein eigenthuemlicher fall von tuberkulose beim rind. Deutsch Z. Tiermed. Pathol. 21:438–454.
Kirkpatrick, B. W., and B. M. Lett. 2018. Short communication: Heritability of susceptibility to infection by *Mycobacterium avium* ssp. *paratuberculosis* in Holstein cattle. J. Dairy Sci. 101:11165–11169. https://doi.org/10.3168/jds.2018-15021.
Kiser, J. N., S. N. White, K. A. Johnson, J. L. Hoff, J. F. Taylor, and H. L. Neibergs. 2017. Identification of loci associated with susceptibility to *Mycobacterium avium* subspecies *paratuberculosis* (Map) tissue infection in cattle. J. Anim. Sci. 95:1080–1091. https://doi.org/10.2527/jas.2016.1152.
Koets, A. P., S. Eda, and S. Sreevatsan. 2015. The within host dynamics of *Mycobacterium avium* ssp. *paratuberculosis* infection in cattle: where time and place matter. Vet. Res. 46:61.
Koets, A. P., G. Adugna, L. G. Janss, H. J. van Weering, C. H. J. Kalis, A. Harbers, V. P. M. G. Rutten, and Y. H. Schukken. (1999) Genetic variation in susceptibility to M. a. paratuberculosis infection in cattle. Pages 169–175 in Proceedings of the Sixth International Colloquium on Paratuberculosis, Melbourne, Australia. International Association of Paratuberculosis Inc., Madison, WI.
Kunkel, S. L., N. W. Lukacs, R. M. Strieter, and S. W. Chensue. 1998. Animal models of granulomatous inflammation. Semin. Respir. Infect. 13:221–228.
Küpper, J., H. Brandt, K. Donat, and G. Erhardt. 2012. Heritability estimates for *Mycobacterium avium* subspecies *paratuberculosis* status of German Holstein cows tested by fecal culture. J. Dairy Sci. 95:2734–2739. https://doi.org/10.3168/jds.2011-4994.
Li, H. 2011. A statistical framework for SNP calling, mutation discovery, association mapping and population genetical parameter estimation from sequencing data. Bioinformatics 27:2987–2993.
Lilenbaum, W., R. Ferreira, C. Dray Marassi, P. Ristow, W. Martins Roland Oelemann, and L. de Souza Fonseca. 2007. Interference of tuberculosis on the performance of ELISAs used in the diagnosis of paratuberculosis in cattle. Braz. J. Microbiol. 38:472–477.
Liontos, L. M., D. Dissanayake, P. S. Ohashi, A. Weiss, L. L. Dragone, and C. J. McGlade. 2011. The Src-like adaptor protein regulates GM-CSFR signaling and monocytic dendritic cell maturation. J. Immunol. 186:1923–1933.
Liu, X., P. Zhang, Y. Bao, Y. M. Han, Y. Wang, Q. Zhang, Z. Z. Zhan, J. Meng, Y. K. Li, N. Li, W. P. J. Zhang, and X. T. Cao. 2013. Zinc finger protein ZBTB20 promotes toll-like receptor-triggered innate immune responses by repressing I kappa B alpha gene transcription. Proc. Natl. Acad. Sci. USA 110:11097–11102.
Loh, P. R., P. Danecek, P. F. Palamara, C. Fuchsberger, Y. A. Reshef, H. K. Finucane, S. Schoenherr, L. Forer, S. McCarthy, G. R. Abecasis, R. Durbin, and A. L. Price. 2016. Reference-based phasing using the Haplotype Reference Consortium panel. Nat. Genet. 48:1443–1448.
Marton, N., E. Baricza, B. Ersek, E. I. Buzas, and G. Nagy. 2015. The emerging and diverse roles of Src-like adaptor proteins in health and disease. Mediators Inflamm. 2015:952536.
McNees, A. L., D. Markesich, N. R. Zayyani, and D. Y. Graham. 2015. *Mycobacterium paratuberculosis* as a cause of Crohn's disease. Expert Rev. Gastroenterol. Hepatol. 9:1523–1534.
Meuwissen, T. H., B. J. Hayes, and M. E. Goddard. 2001. Prediction of total genetic value using genome-wide dense marker maps. Genetics 157:1819–1829.
Meyer, K. 2007. WOMBAT: A tool for mixed model analyses in quantitative genetics by restricted maximum likelihood (REML). J. Zhejiang Univ. Sci. B 8:815–821.
Milner, A. R., A. W. D. Lepper, W. N. Symonds, and E. Gruner. 1987. Analysis by Elisa and Western blotting of antibody reactivities in cattle infected with *Mycobacterium paratuberculosis* after absorption of serum with M-Phlei. Res. Vet. Sci. 42:140–144.
Montero-Meléndez, T, X Llor, E García-Planella, M Perretti, and A Suárez. (2013). Identification of novel predictor classifiers for inflammatory bowel disease by gene expression profiling. PLoS One 8:e76235. https://doi.org/10.1371/journal.pone.0076235.
Mucha, R., M. R. Bhide, E. B. Chakurkar, M. Novak, and I. Mikula. 2009. Toll-like receptors TLR1, TLR2 and TLR4 gene mutations and natural resistance to *Mycobacterium avium* subsp. *paratuberculosis* infection in cattle. Vet. Immunol. Immunopathol. 128:381–388. https://doi.org/10.1016/j.vetimm.2008.12.007.
Neibergs, H. L., M. L. Settles, R. H. Whitlock, and J. F. Taylor. 2010. GSEA-SNP identifies genes associated with Johne's disease in cattle. Mamm. Genome 21:419–425.
Oo, H. Z., K. Sentani, N. Sakamoto, K. Anami, Y. Naito, N. Uraoka, T. Oshima, K. Yanagihara, N. Oue, and W. Yasui. 2014. Overexpression of ZDHHC14 promotes migration and invasion of scirrhous type gastric cancer. Oncol. Rep. 32:403–410. https://doi.org/10.3892/or.2014.3166.
Osterstock, J. B., G. T. Fosgate, B. Norby, E. J. Manning, M. T. Collins, and A. J. Roussel. 2007. Contribution of environmental mycobacteria to false-positive serum ELISA results for paratuberculosis. J. Am. Vet. Med. Assoc. 230:896–901.
Pant, S. D., F. S. Schenkel, C. P. Verschoor, Q. You, D. F. Kelton, S. S. Moore, and N. A. Karrow. 2010. A principal component regression based genome wide analysis approach reveals the presence of a novel QTL on BTA7 for MAP resistance in holstein cattle. Genomics 95:176–182. https://doi.org/10.1016/j.ygeno.2010.01.001.
Park, H. T., and H. S. Yoo. 2016. Development of vaccines to *Mycobacterium avium* ssp. *paratuberculosis* infection. Clin. Exp. Vaccine Res. 5:108–116. https://doi.org/10.7774/cevr.2016.5.2.108.
Piepoli, A., O. Palmieri, R. Maglietta, A. Panza, E. Cattaneo, A. Latiano, E. Laczko, A. Gentile, M. Carella, G. Mazzoccoli, N. Ancona, G. Marra, and A. Andriulli. 2012. The expression of leucine-

rich repeat gene family members in colorectal cancer. Exp. Biol. Med. (Maywood) 237:1123–1128. https://doi.org/10.1258/ebm.2012.012042.

Prosser, D. C., D. Tran, A Schooley, B. Wendland, and J.K. Nqsee. 2010. A novel, retromer-independent role for sorting nexins 1 and 2 in RhoG-dependent membrane remodeling. Traffic 11:1347–1362. https://doi.org/10.1111/j.1600-0854.2010.01100.x.

Ran, C., and A. Belin. 2014. The genetics of Parkinson's disease: Review of current and emerging candidates. Journal of Pankinsonism and Restless Legs Syndrome 4:63–75. https://doi.org/10.2147/JPRLS.S38954.

Rathnaiah, G., D. K. Zinniel, J. P. Bannantine, J. R. Stabel, Y. T. Grohn, M. T. Collins, and R. G. Barletta. 2017. Pathogenesis, molecular genetics, and genomics of *Mycobacterium avium* ssp. *paratuberculosis*, the etiologic agent of Johne's disease. Front. Vet. Sci. 4:187.

Richardson, E.., and S. J. More. 2009. Direct and indirect effects of Johne's disease on farm and animal productivity in an Irish dairy herd. Ir. Vet. J. 62:526–532. https://doi.org/10.1186/2046-0481-62-8-526.

Ring, S. C., D. C. Purfield, M. Good, P. Breslin, E. Ryan, A. Blom, M. L. Doherty, D. G. Bradley, and D. P. Berry. 2019. Variance components for bovine tuberculosis infection and multi-breed genome-wide association analysis using imputed whole genome sequence data. PLoS One 14:e0212067. https://doi.org/10.1371/journal.pone.0212067.

Robertson, A., and I. M. Lerner. 1949. The heritability of all-or-none traits: Viability of poultry. Genetics 34:395–411.

Ross, R., and L. Agius. 1992. The process of atherogenesis—Cellular and molecular interaction—From experimental animal-models to humans. Diabetologia 35:S34–S40.

Sargolzaei, M., J. P. Chesnais, and F. S. Schenkel. 2014. A new approach for efficient genotype imputation using information from relatives. BMC Genomics 15:478.

Schaefer, C. F., K. Anthony, S. Krupa, J. Buchoff, M. Day, T. Hannay, and K. H. Buetow. 2009. PID: The Pathway Interaction Database. Nucleic Acids Res. 37:D674–D679.

Settles, M., R. Zanella, S. D. McKay, R. D. Schnabel, J. F. Taylor, R. Whitlock, Y. Schukken, J. S. Van Kessel, J. M. Smith, and H. Neibergs. 2009. A whole genome association analysis identifies loci associated with *Mycobacterium avium* ssp. *paratuberculosis* infection status in US Holstein cattle. Anim. Genet. 40:655–662.

Strandén, I., and M. Lidauer. 1999. Solving large mixed linear models using preconditioned conjugate gradient iteration. J. Dairy Sci. 82:2779–2787.

Strandén, I., and E. A. Mäntysaari. 2010. A recipe for multiple trait deregression. Interbull Bull. 42:21–24.

Sweeney, R. W., M. T. Collins, A. P. Koets, S. M. McGuirk, and A. J. Roussel. 2012. Paratuberculosis (Johne's disease) in cattle and other susceptible species. J. Vet. Intern. Med. 26. https://doi.org/10.1111/j.1939-1676.2012.01019.x.

Twomey, A. J., R. G. Sayers, R. I. Carroll, N. Byrne, E. O. Brien, M. L. Doherty, J. C. McClure, D. A. Graham, and D. P. Berry. 2016. Genetic parameters for both a liver damage phenotype caused by *Fasciola hepatica* and antibody response to *Fasciola hepatica* phenotype in dairy and beef cattle. J. Anim. Sci. 94:4109–4119.

VanRaden, P. M. 2008. Efficient methods to compute genomic predictions. J. Dairy Sci. 91:4414–4423.

VanRaden, P. M., and A. H. Sanders. 2003. Economic merit of crossbred and purebred US dairy cattle. J. Dairy Sci. 86:1036–1044.

Varges, R., C. Dray Marassi, W. Oelemann, and W. Lilenbaum. 2009. Interference of intradermal tuberculin tests on the serodiagnosis of paratuberculosis in cattle. Res. Vet. Sci. 86:371–372.

Vigetti, D., A. Genaseetti, E. Karousou, M. Viola, P. Moretto, M. Clerici, S. Deleonibus, G. De Luca, V. C. Hascall, and A. Passi. 2010. Proinflammatory cytokines induce hyaluronan synthesis and monocyte adhesion in human endothelial cells through hyaluronan synthase 2 (HAS2) and the nuclear factor-kappaB (NF-kappaB) pathway. J. Biol. Chem. 285:24639–24645. https://doi.org/10.1074/jbc.M110.134536.

Windsor, P. A., and R. J. Whittington. 2010. Evidence for age susceptibility of cattle to Johne's disease. Vet. J. 184:37–44.

Wray, N. R., J. Yang, M. E. Goddard, and P. M. Visscher. 2010. The genetic interpretation of area under the ROC curve in genomic profiling. PLoS Genet. 6:e1000864.